



The ExoMars Schiaparelli Entry, Descent and Landing Demonstrator Module (EDM) System Design

Andrew J. Ball¹ · Thierry Blancquaert¹ · Olivier Bayle¹ · Leila V. Lorenzoni¹ · Albert F.C. Haldemann¹ · the Schiaparelli EDM team²

Received: 5 January 2020 / Accepted: 27 January 2022 / Published online: 27 July 2022
© The Author(s) 2022

Abstract

The Entry, Descent and Landing Demonstrator Module (EDM) named Schiaparelli, was the ESA-led Mars lander element of the ESA-Roscosmos ExoMars 2016 mission. Following launch on 14 March 2016 with the ExoMars Trace Gas Orbiter (TGO) and cruise to Mars, Schiaparelli separated for encounter with Mars to demonstrate entry, descent and landing technologies. Although on 19 October 2016 the final touchdown and surface operation were not achieved, other aspects were demonstrated and reported via real-time telemetry transmitted at 8 kbps in UHF during entry and descent.

This paper presents a technical description of the elements of the Schiaparelli EDM system and its operation, plus reference to published post-flight analyses of the data obtained.

Keywords Mars · Spacecraft · Landers · Entry, Descent and Landing (EDL) · ExoMars · Schiaparelli

1 Introduction

Schiaparelli originated from the ExoMars programmatic objective for the development, in-flight and *in situ* demonstration of Entry, Descent and Landing (EDL) of a payload on the surface of Mars. In 2009, ExoMars was split into two missions: the first, for launch in 2016, to include a Mars orbiter for science and data relay; the second to include the ExoMars Rover with its Pasteur Payload. Since the landing system of the Rover mission was conceived to be led by an international partner (initially NASA, then later Roscosmos), the desire to retain the EDL demonstration objective for implementation by Europe led to the decision to embark an ‘EDL Demonstrator Module’ (EDM) on the 2016 Trace Gas Orbiter (TGO). Several elements of the EDM were derived from those already under development for the landing platform of the original ExoMars mission architecture. Emerging from industrial

ExoMars-16
Edited by Håkan Svedhem and Christopher T. Russell

✉ A.J. Ball
andrew.ball@esa.int

¹ ESA ESTEC, Noordwijk, The Netherlands

² <http://www.esa.int/exomars>

studies in mid-2009 were ‘large’ (550–600 kg entry mass) and ‘small’ (~300 kg) options, from which the larger option was selected. The EDM was to be separated from the TGO 3 days prior to Mars arrival on a hyperbolic approach trajectory and (following wake-up from hibernation during the coasting phase) enter the martian atmosphere, transmitting essential, real-time telemetry via UHF to the TGO and (after touchdown) also to other Mars Orbiters for relay of its data to Earth.

Although for some time during development the possibility to include a Radioisotope Thermoelectric Generator (RTG) power source and Radioisotope Heater Unit (RHU)-supported thermal control (thus enabling long-duration surface operations) was studied in co-operation with Roscosmos, the initial concept—and indeed final configuration—was foreseen for operations on Mars of only a few sols, based on the electrical energy of on-board batteries. Long-duration surface operations (as might be afforded by an RTG or solar arrays) were not necessary for achieving the defined programmatic objectives of EDL demonstration. Note that solar array power would also have been vulnerable to the possibility of dust storms at the time of arrival, at a solar longitude of 244.7°, during the statistical dust storm season.

Agency reviews were held as part of the overall ExoMars 2016 mission system reviews as follows:

- Preliminary Design Review (PDR): Oct–Dec 2010;
- Critical Design Review (CDR): Oct 2013–Apr 2014;
- Qualification and Acceptance Review (QAR), combining Qualification Review and Flight Acceptance Review: Aug–Oct 2015.

Lessons learned from *Beagle 2* and recommendations from its commission of enquiry were applied at programmatic, mission system and technical levels, and the status with respect to the recommendations was assessed at each agency-level review.

The EDM was named Schiaparelli in November 2013 in honour of the Italian astronomer Giovanni Schiaparelli.

The Schiaparelli industrial consortium was led by Thales-Alenia Space Italy (TAS-I) in Turin and included the partners / suppliers listed in the [Appendix](#).

In addition, several elements of payload were provided via ESA as ‘Customer-Furnished Items’ (CFI):

- COMARS+ entry sensors (DLR and CNES);
- DeCa descent camera (ESA);
- DREAMS surface environmental sensors package (ASI), selected via an Announcement of Opportunity.
- INRRI optical retroreflector (ASI).

2 Overall Configuration

Figure 1 shows the overall external configuration of Schiaparelli for Mars atmospheric entry (minus thermal blanket). The 2.4 m diameter module has a 70° sphere-cone Front Shield (FS) with 600 mm nose radius, and a truncated conical Back Shell (BSH) with 47° cone angle. The aeroshell shape was selected as the lowest risk option, based on the extensive proven heritage at Mars from *Viking* onwards, plus previous European experience including *NetLander*. The diameter was reduced from the 3.4 m foreseen for the original ExoMars configuration (landing platform + rover).

Schiaparelli was mounted on the TGO via the Main Separation Assembly (MSA), which interfaced to recessed brackets at three positions in the back cover, and on the TGO side on

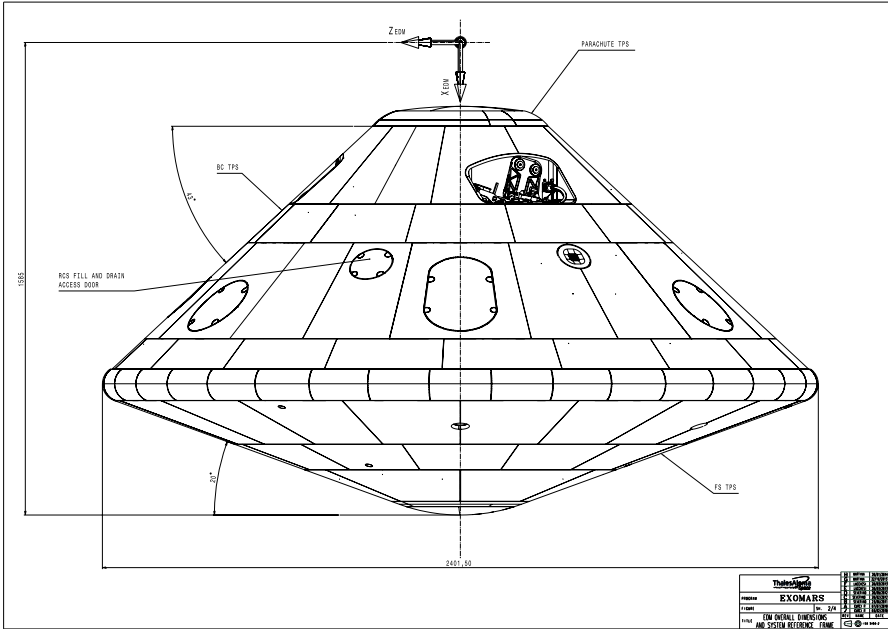


Fig. 1 Overall dimensions and system reference frame of Schiaparelli (including Thermal Protection System (TPS) tiling but excluding Front Shield Multi-Layer Insulation (MLI) and Back Cover Single-Layer Insulation (SLI)). The MSA interface that remained on Schiaparelli after separation is visible in the recess (1 of 3 identical) on the back cover. Also visible just below this is the Sun Detection Sensor (SDS). Credit: TAS-I

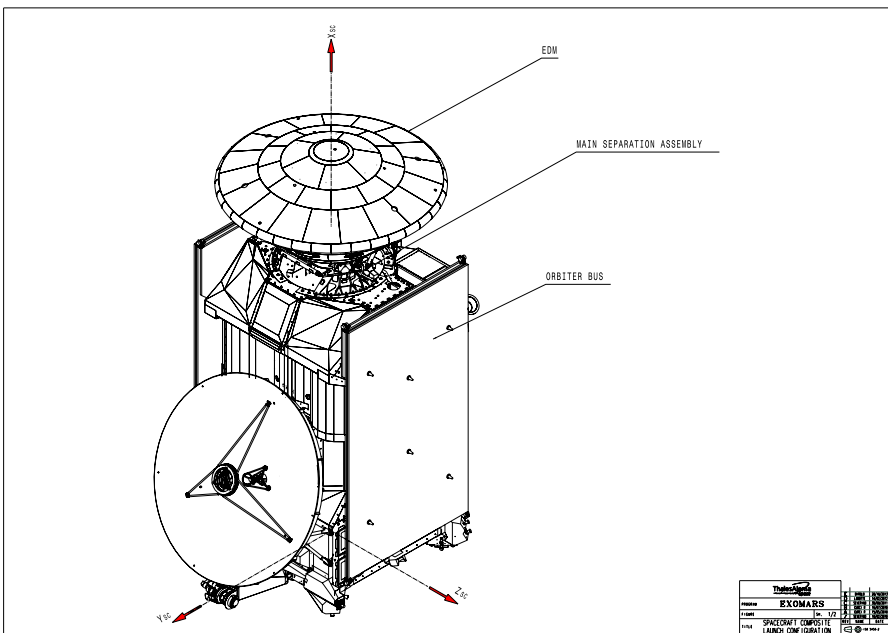


Fig. 2 Accommodation of Schiaparelli on the TGO (launch configuration). The mechanical loads of Schiaparelli are transferred via the MSA to the TGO central tube. Credit: TAS-I



Fig. 3 Main Separation Assembly (MSA), including the interface fittings that remained on the EDM after separation. The EDM is above and TGO is below in the view shown. The separation plane is between the cyan and magenta parts shown above. Each of the three separation mechanisms used a spring release, initiated via a Non-Explosive Actuator (NEA), and incorporated a 128-pin umbilical separation connector. For further details, see Caldirola et al. (2015). Credit: TAS-I/RUAG

the top deck above the 591 mm-radius central tube of the primary structure (Fig. 2). The MSA (Fig. 3) supported Schiaparelli for launch and cruise, provided routing for electrical harness, and provided the necessary electrical and mechanical separation on approach to Mars. The total MSA mass was 39.3 kg, of which 30.3 kg remained on the TGO after separation.

The nominal relative delta-V of separation was 0.32 m s^{-1} , with a nominal rotation rate of 2.70 rpm for spin stabilisation. This was within a range specified between a minimum of 2.5 rpm (to guarantee exo-atmospheric stability) and a maximum of 3.0 rpm (driven by the need to allow aerodynamic torques to orient the probe to maintain a low angle of attack at peak heating). The spin was imparted by the angled MSA mechanism rather than spinning the whole composite.

Figure 4 shows an exploded view of the main elements of Schiaparelli.

The conical element of the BSH, called the Back Cover (BCV), is made from aluminium honeycomb with CFRP skins. The BCV incorporates cut-outs for the three Main Separation Mechanism (MSM) brackets (i.e. interface to the MSA), access doors, fill & drain valves, venting, Sun Detection Sensor and UHF antenna. The BCV is connected to the FS structure via the 6-point Front Shield Separation Mechanism (FSSM). Inside the BCV, 12 struts (6 bipods) carry loads between the Surface Platform and Upper Ring (around the parachute cover), and between the Surface Platform and MSM brackets; six struts connect the Up-

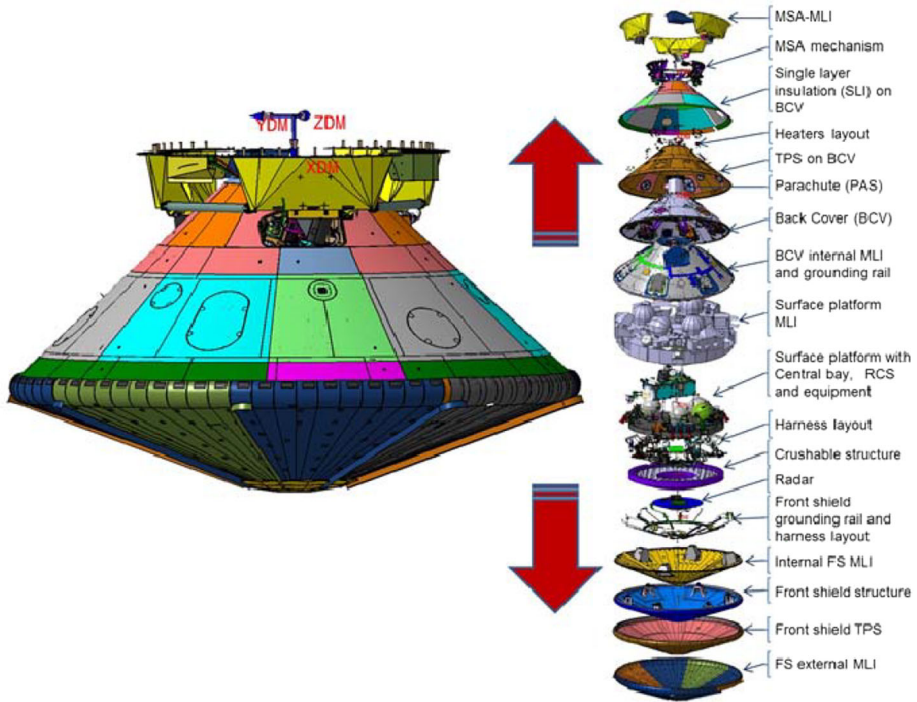


Fig. 4 Exploded view of the Schiaparelli EDM, attached to the Main Separation Assembly (MSA). Credit: TAS-I

per Ring with the six-point Surface Platform Separation Mechanism (SPSM) around the perimeter of the Surface Platform, while each of the three MSM brackets is connected with two shorter struts to adjacent pairs of SPSMs. There are two types of SPSM (arranged alternately around the perimeter); three with the spring-actuated separation mechanism and three carrying electrical connector interfaces (Prieto et al. 2013).

A cross-section of Schiaparelli is shown in Fig. 5. It should be noted that no redundancy was incorporated in the design, except where specified by the relevant standard (e.g. CAN Bus and pyro lines).

The as-flown entry mass of Schiaparelli was 576.3 kg. Table 1 gives a mass breakdown. The nominal EDL sequence for Schiaparelli is shown in Fig. 6.

3 Heatshield and Entry Parameters

A tiled Norcoat[®] Liège Thermal Protection System (TPS), bonded with silicone adhesive ESP495, covers both FS and BSH. The FS TPS comprises a central dome tile, surrounded by a ring tile, 3 rows of tiles on the conical section (of 6, 12 and 18 tiles, respectively) and finally a row of trailing edge tiles. The BSH TPS comprises a parachute break-out patch at the apex and 4 rows of tiles on the conical section.

The FS TPS incorporates:

- 9 penetrations for MLI grounding;
- 4 closing plugs at ground handling attachment points (clearly visible in Fig. 8a);

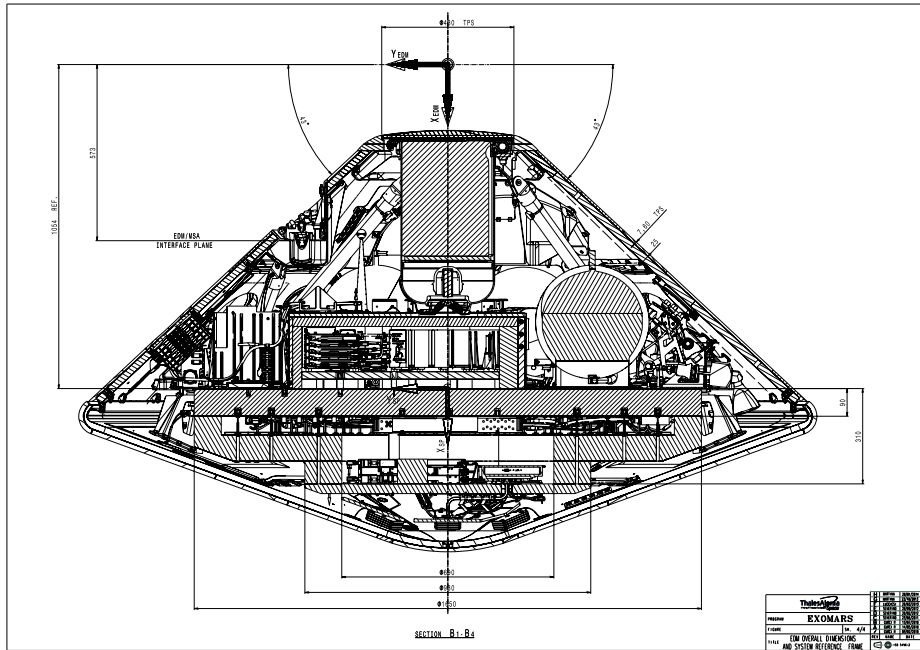


Fig. 5 Schiaparelli cross-section. Credit: TAS-I

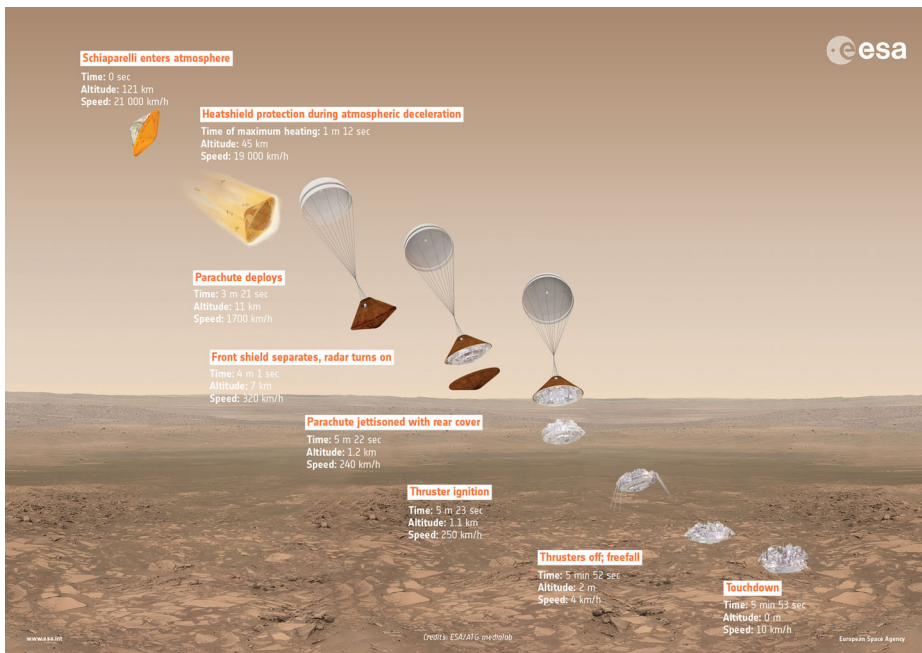


Fig. 6 Schiaparelli nominal EDL sequence. Copyright: ESA/ATG medialab

Table 1 Schiaparelli mass breakdown (simplified w.r.t. original project documentation)

Element	Item	Mass/kg	Comment
Back Shell	Structure, separation mechanisms, venting box, fixation h/w	99.0	
	TPS	26.2	Includes TPS on parachute break-out patch
	Thermal control	4.1	
	Parachute System	25.9	Excludes TPS on break-out patch
	Sun Detection Sensor (SDS)	0.05	
	UHF Antenna	1.0	
	Harness and grounding	2.9	Includes RF co-ax; excludes harness considered as part of payload
	Payload	4.8	COMARS+; Thermocouples & Thermistors incl. harness
	<i>Subtotal</i>	<i>163.97</i>	<i>Value used in Flight Dynamics Database (sum of Back Shell (not ablated), BoP + bag, PAS(bag), canopy & lines</i>
	Front Shield	Structure, separation mechanism, fixation h/w, bioseal, attachment for MLI	42.4
TPS		37.0	
Thermal Control		5.8	Includes MLI
Harness and grounding		0.2	Excludes harness considered as part of payload
Payload		4.6	Pressure sensors, thermocouples and thermistors
FS Ballast		22.0	Tungsten alloy blocks
<i>Subtotal</i>		<i>112.07</i>	<i>Value used in Flight Dynamics Database</i>

Table 1 (Continued)

Element	Item	Mass/kg	Comment
Surface Platform-Propulsion Bay	Surface Platform Propulsion Bay: structure, crushable material, separation mechanisms, fixation h/w	53.6	Includes 13.8 kg crushable material
	Reaction Control System (dry)	65.6	Includes secondary structures for engines and tanks
	SP Propulsion Bay Thermal Control	12.7	Includes 1.38 kg thermal capacitor for MIMU
	RTPU (NL) battery	16.8	
	RTPU (HR) battery	3.0	
	Remote Terminal and Power Unit (RTPU)	5.4	
	MIMU	4.8	Excludes thermal capacitor
	Radar Doppler Antenna (RDA)	15.4	Includes circular support panel
	SP Propulsion Bay Harness and grounding	14.1	Excluding landing accelerometers and associated harness counted as payload
	SP Propulsion Bay Payload	1.3	DeCa, DeCa support bracket, landing accelerometers and associated harness
Surface Platform-Central Bay (CB)	SP Ballast	10	Tungsten alloy blocks
	Propellant	46.2	15.4 kg hydrazine in each of 3 tanks; predicted remaining propellant at touchdown was 20.9 kg.
	Pressurant	0.4	Helium
	<i>Subtotal</i>	<i>249.3</i>	<i>Wet mass including payload and ballast</i>
	Surface Platform Central Bay Structure	15.4	Includes insulating foam, connector plates, stand-offs, cooling pipes and fixation h/w.
	CTPU (NL) battery	12.0	Inside CB warm compartment
Central Terminal and Power Unit (CTPU)	4.9	Inside CB warm compartment	
CTPU thermal capacitor	4.3	Inside CB warm compartment	
CTPU Relay Box	1.4	On top of CB	
RTPU Relay Box	1.4	On top of CB	
UHF Transceiver + Switch	1.7	Inside CB warm compartment	
UHF Transceiver thermal capacitor	1.9	Inside CB warm compartment	
UHF Surface Platform Helix Antenna	1.6	On top of CB	
Harness and grounding	2.0	Includes RF co-ax	
Central Bay Payload	4.4	DREAMS + INRRI	
<i>Subtotal</i>	<i>51.0</i>	<i>Including payload</i>	

Table 1 (Continued)

Element	Item	Mass/kg	Comment
Surface Platform	Subtotal	300.26	Wet mass including payload and ballast, value used in Flight Dynamics Database
	Total at entry, as flown	576.3	From Flight Dynamics Database. Back Shell + Front Shield + Surface Platform
	Main Separation Assembly - part remaining on TGO	30.3	

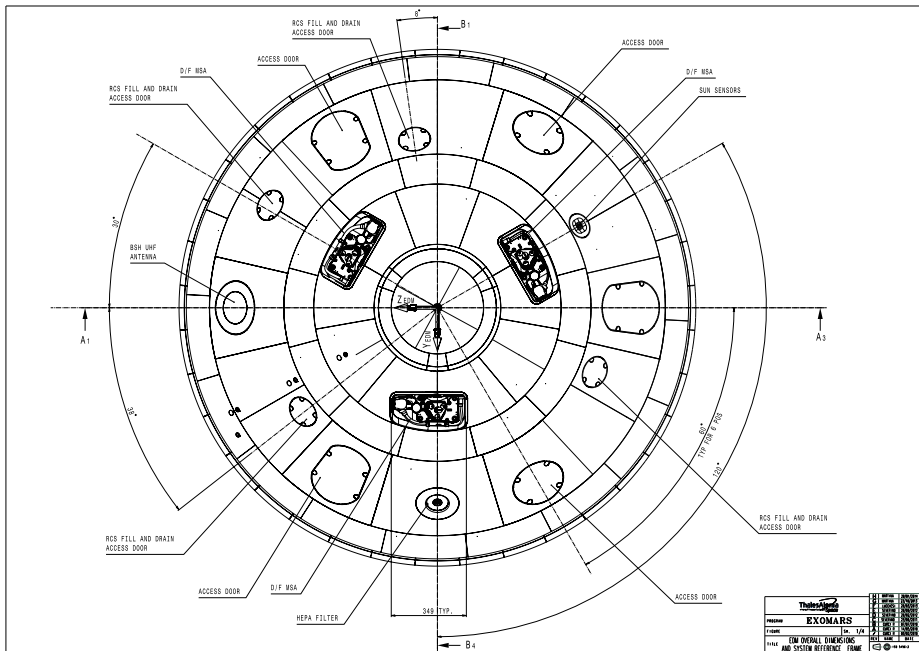


Fig. 7 Back Shell layout with TPS tiles, showing the parachute break-out patch, MSA interface points, access doors, UHF antenna, Sun Detection Sensor and venting. Also visible in the lower left quadrant are the locations of the COMARS+ sensor heads, COMARS+ radiometer and the three Back Shell TPS thermocouple plugs. Credit: TAS-I

- 7 thermal plugs for FS sensors, and
- 4 pressure sensor inlet holes.

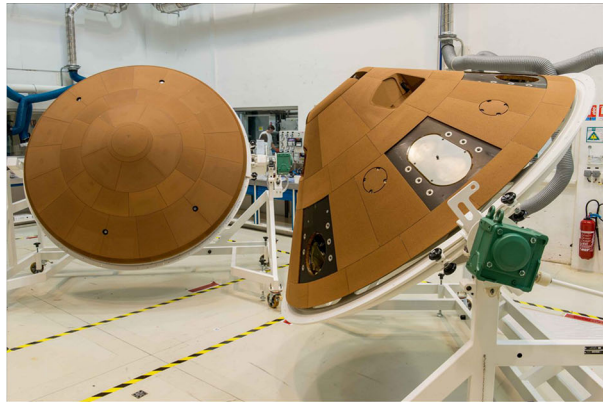
The BSH TPS incorporates:

- 24 penetrations for SLI grounding;
- 3 penetrations for attachment to the MSA;
- one break-out patch for the parachute;
- 6 access doors (one of which is closed by a patch holding the UHF antenna under an RF-transparent Norcoat® 4011 TPS patch);
- 4 access doors for fill and drain of the RCS (propellant tanks and pressurant tank);
- Venting box (a HEPA filter not being used, finally);
- Sun Detection Sensor (see GNC section);
- 3 thermal plugs;
- 4 COMARS+ sensor locations.

Figures 7 and 8 show the BSH and FS layouts.

Entry parameters are summarised in Table 2, and more information on the thermal aspects is available in Perotto et al. (2017).

Fig. 8 Views of the Schiaparelli Front and Back Heat Shield TPS during assembly. Copyright: Airbus Defence and Space SAS 2014 A. Gilbert. The images are available on the ESA Exploration web site <http://exploration.esa.int/>



a



b

4 GNC

The Schiaparelli GNC architecture was based around an inertial measurement unit (Honeywell MIMU), supplemented with a Sun Detection Sensor (a TNO Mini-FSS) in the Back Shell, and, following FS separation, a four-beam Radar Doppler Altimeter (RDA). During coasting hibernation the IMU was powered off; attitude reconstruction on exit from hibernation was performed based on SDS data.

The RDA operated at 35.76 GHz. Three beams 120° apart in azimuth were angled 20° off-nadir from a central beam. A field test campaign was performed for characterisation of the RDA performance.

Note that the final freefall would have been from 1.8 m following cut-off of the RCS; actual touchdown would thus have been open-loop, the landing deceleration being measured by both the IMU and landing accelerometers (4 s of sampling from RCS OFF).

See Amelio et al. (2016) for details of the avionics and GNC architecture, and Bombaci et al. (2016) for a description of the RDA.

5 Parachute System

The Schiaparelli Parachute System (PAS) comprised a nylon Disk-Gap-Band (DGB) parachute, its deployment bag, the Parachute Deployment Device (PDD) mortar and the

Table 2 Summary of Schiaparelli entry parameters (format adapted from Davies and Arcadi 2006)

Trajectory	Geometry			Aero/thermal		TPS	
	Entry flight path angle	Shape	70° sphere-cone	Trim L/D (specify trim α)	Ballistic (0° average)	Material designation	Norcoat® Liège
Inertial entry velocity	-12.48° @ 120 km (post-flight) 6.03 km s ⁻¹	Nose radius	0.6 m	Ballistic co-eff.	75.2 kg m ⁻² at peak heat flux	Thickness	Front Shield: 12.2 mm (nose) increasing to 15.4 mm (FS trailing edge) Back cover: 7.6 mm
Relative entry velocity	5.79 km s ⁻¹	Base area	4.53 m ²	Stagnation heating rate	582 kW m ⁻² (Sutton-Graves correlation, predicted)	Ablating? Ejected?	Yes Yes
Velocity at peak heat	5.09 km s ⁻¹	Vehicle mass	576.3 kg	Integrated heat load	34 MJ m ⁻² (predicted)	Resin material	Phenolic
Control method	Ballistic	TPS mass fraction, incl. insulation	0.11	Peak radiative heat flux	123 kW m ⁻² (predicted)	Matrix material	Cork
Centre of Gravity X _{CG/D}	0.247	Payload mass	15.2 kg	Peak Heating stagnation pressure	11 kPa	Total material density	420 kg m ⁻³ (nominal, outgassed)

Fig. 8 (Continued)



c

PAS cover, referred to as the Break-out-Patch (BoP) when covered with TPS, and a 1.83 m diameter BoP drogue parachute. The PAS is shown in cross-section in Fig. 5. The main parachute has a diameter 12 m with a geometric porosity of 22.4%, scaled from the Huygens second stage parachute (see Fig. 9). The parachute was designed to decelerate Schiaparelli from up to Mach 2.1 (nominally 1.95 ± 0.15 , 3σ) to a sub-sonic speed compatible with Surface Platform separation, and to achieve a flight path angle $< -87^\circ$ at a height above ground > 1.4 km. The parachute was design to inflate under dynamic pressure at deployment between 632 and 928 Pa (in the probe's wake). The design maximum load limit was 75 kN.

The three parachute bridles are attached to the BCV Upper Ring.

Final functional and structural qualification of the Schiaparelli parachute was conducted at NASA Ames' NFAC facility.

6 Surface Platform

The need to support EDL functions until touchdown, and then maintain operations on Mars for the relay of the full EDL dataset and science data, gave rise to a Surface Platform de-

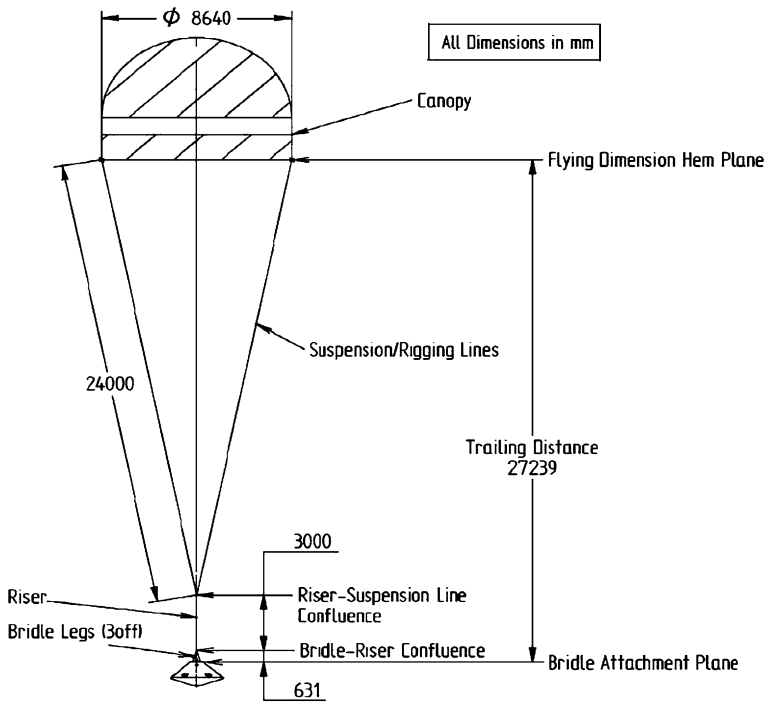


Fig. 9 Schiaparelli parachute in deployed configuration. Credit: TAS-I

sign based around a circular baseplate carrying both EDL elements ('Propulsion Bay') and a warm compartment ('Central Bay'). Mounted underneath the baseplate are the RTPU, the crushable structure for touchdown, and the RDA (circular support panel carrying electronics unit, RF network and 4 antennas). Crushable structure was selected for the landing technology following a trade-off (in 2010 prior to System PDR) vs. landing legs, vented airbags and non-vented airbags. Although legs or vented airbags could be valid alternatives, crushable structure was found to be the simplest solution for the mission objectives. The core of the crushable structure is an aluminium honeycomb (Alcore 3/8-5052-0.0007 1.0) with crushing strength 0.17 MPa. The maximum axial quasi-static deceleration load experienced by equipment on the Surface Platform was expected to be approximately 48 g.

After the touchdown phase only the Central Bay was needed to remain active to continue operations. Figures 10 and 11 show the layout of the Surface Platform.

7 Reaction Control System

Hydrazine monopropellant was stored in three 17.5 l tanks (incorporating diaphragms for propellant management), supplying three clusters (120° apart) of three CHT 400N pulsed engines (nozzles canted 18° outboard from nadir, with the outer pair of each cluster tilted by 13° for roll control). The system was pressurized from a 15.6 l He tank. A schematic of the RCS is shown in Fig. 12.

With respect to the as-built configuration, pressure sensors were removed in Baikonur due to a late concern about welds. This represented a minor reduction in the data available for post-flight analysis rather than a performance loss.

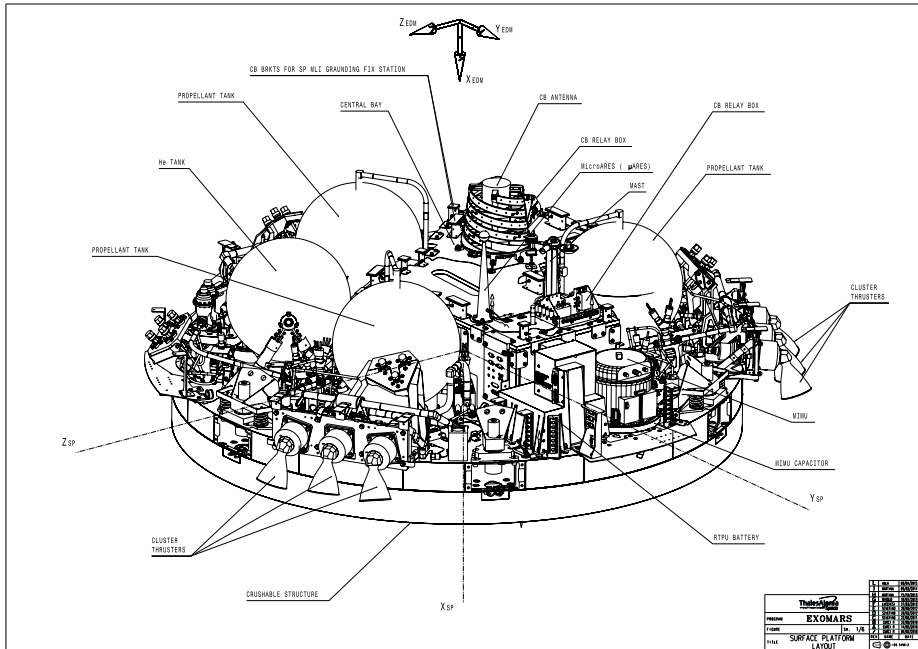


Fig. 10 Schiaparelli Surface Platform (viewed without thermal blanket). Credit: TAS-I

8 Thermal Design

Schiaparelli's thermal design had to cope with the variable thermal environments during the various phases of the mission from launch to the surface of Mars, including a 72 hours coasting phase between separation from TGO and atmospheric entry. See Perotto et al. (2017) for details of the design and of its performance in flight.

For cruise, passive thermal control employed SLI and MLI on the FS and BSH interior and exterior, and on the exterior of the surface platform. Active thermal control was used when needed by means of heaters, powered during cruise from TGO, then from the on-board batteries after separation (controlled by a mix of thermostats (for within the Central Bay) and the Thermal Control System (TCS) in the CTPU).

The Central Bay warm compartment employed passive thermal design elements in addition to the battery-powered heaters: polyimide foam insulation (sides and top), and a gas gap with standoffs below the support plate.

Thermal boosts were implemented before separation from TGO (to minimise electrical heating energy needed from the Schiaparelli batteries during coast) and another just before entry (mostly to warm up the RCS).

Thermal capacitors (using wax phase change material – see Gottero et al. 2014) were accommodated under the MIMU (97 kJ), CTPU (216 kJ) and UHF Transceiver (149 kJ) to prevent overheating from the heat dissipated from these units during cruise and EDL, and for the CTPU and Transceiver also during the surface phase; the stored dissipated heat from these units could be released during periods of low dissipation to support heating of the warm compartment.

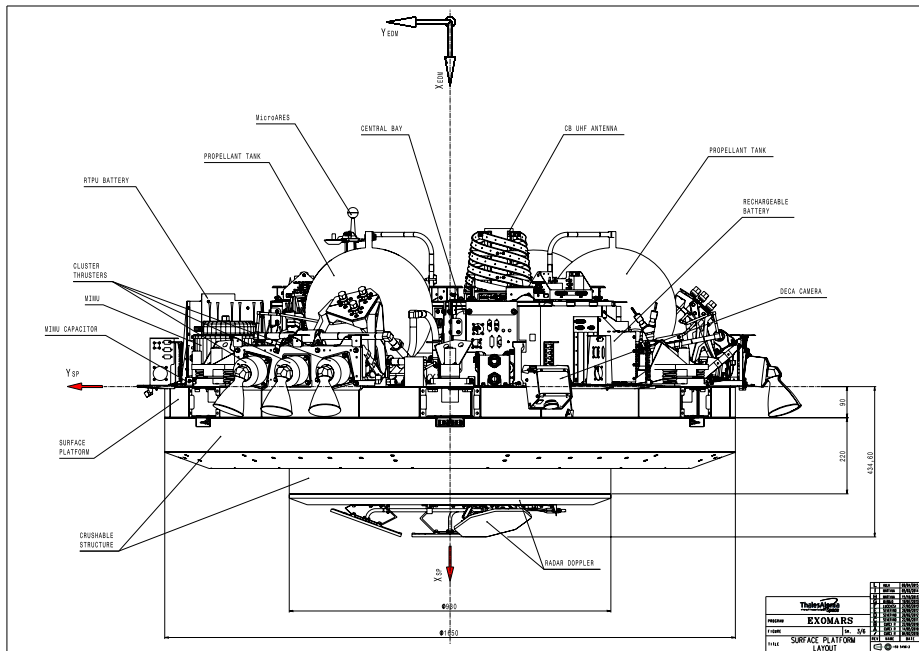


Fig. 11 Side view of the Surface Platform. Credit: TAS-I

EDM-level verification by thermal vacuum / thermal balance test was only for the cruise, coast and thermal boost (under vacuum), while for EDL and surface phase the verification was only by analysis. See Gottero et al. (2016) for more detail.

9 Planetary Protection

Schiaparelli was classified as Planetary Protection Category IVa, being a landed system neither carrying life-detection equipment nor accessing a ‘Special Region’ of Mars. The following bioburden requirements were thus applied (vs. values achieved at launch):

- total (Encapsulated and Surface) bioburden of less than 5×10^5 spores; (achieved at launch: 291601 spores)
- less than 3×10^5 spores on exposed internal and external surfaces; (achieved at launch: 151360 spores)
- less than 300 spores/m² average on exposed internal and external surfaces. (achieved at launch: 73 spores/m²)

DHMR was used on hardware shown to be compatible with that sterilization process, and sterile IPA 70% was used to maintain surface bioburden density below acceptable levels. Integration of Schiaparelli was performed in an ISO 7 Highly Controlled facility (ISO7HC).

An airtight bioseal ring was implemented between the BCV and FS to guard against contamination during integration activities with closed heatshield in facilities outside of ISO7HC. This bioseal had the additional design role to help prevent incursion of hot gases during entry.

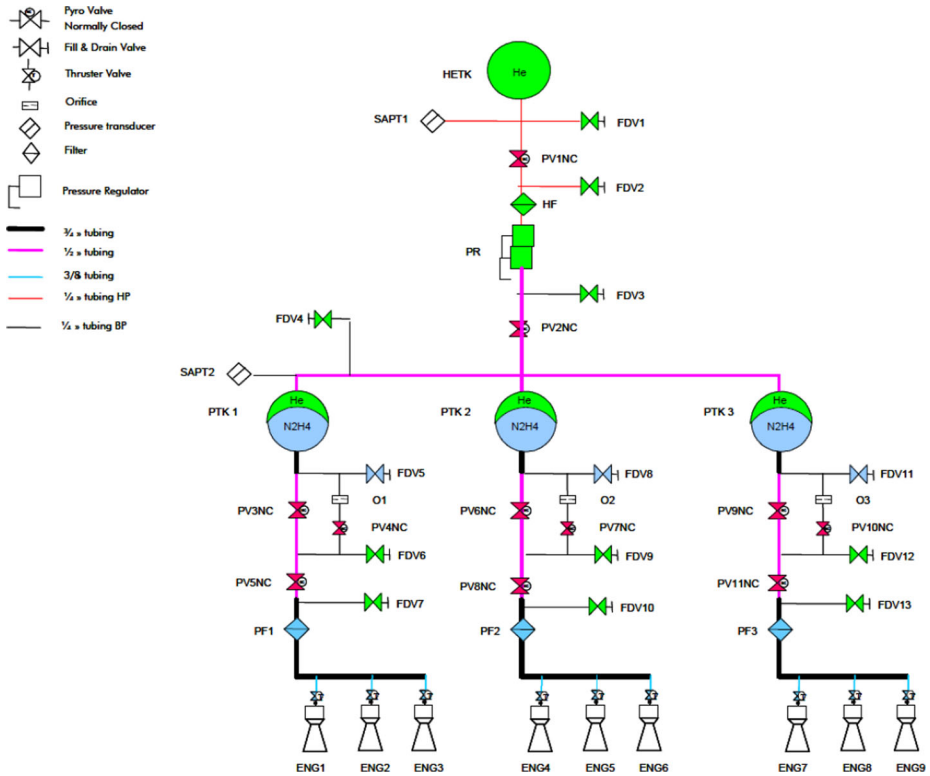


Fig. 12 Schiaparelli Reaction Control System overview. Credit: TAS-I

The initial design included a HEPA filter for venting during launch but problems with its performance venting air with ambient humidity at low pressures led to its replacement with a simpler venting box design (HEPA filter Structural Model housing, with steel wool packed inside) while still maintaining acceptable bioburden levels and thermo-fluidic performance during ascent and entry.

10 Electrical Power

During cruise, Schiaparelli was powered from the TGO unregulated bus (routed via the MSA and RTPU). After separation from TGO, electrical power for Schiaparelli was provided by three batteries (charged during cruise):

- CTPU (NL) battery mounted inside the Central Bay, using ABSL 18650NL Li-ion cells in 8s27p configuration (nominal capacity 62.1 Ah) to supply a 28V unregulated bus;
- RTPU (NL) battery for EDL phase only, mounted externally, using ABSL 18650NL Li-ion cells in 8s38p configuration (nominal capacity 87.4 Ah) to supply a 28V unregulated bus;
- RTPU (HR) battery for high rate needs during EDL (separation pyros, parachute deployment device, RCS valves, heaters), using ABSL 18650HR Li-Ion cells in 15s3p configuration (nominal capacity 3.3 Ah) to supply a 60 V unregulated bus.

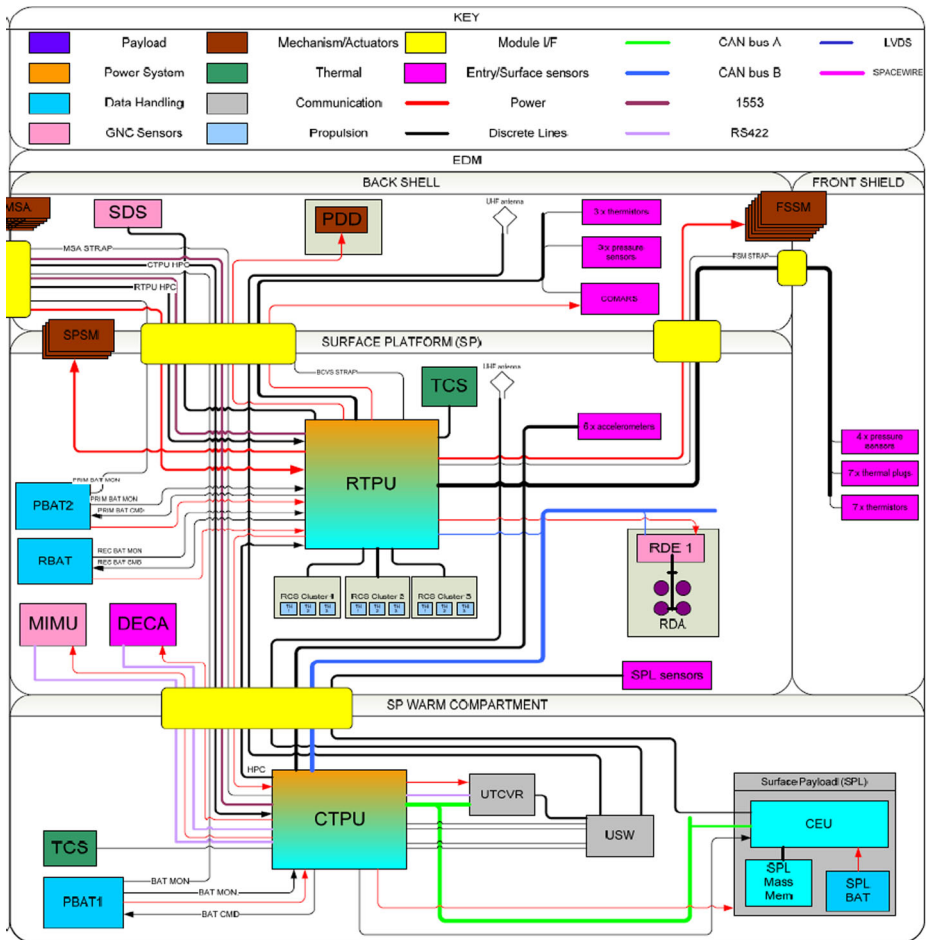


Fig. 13 Schiaparelli Avionics subsystem block diagram. UTCVR = UHF Transceiver; USW = UHF Switch; PBAT1 = CTPU (NL) Battery; PBAT2 = RTPU (NL) Battery; RBAT = RTPU (HR) Battery; RDE = RDA Drive Electronics. Credit: TAS-1

The electrical power system is described in more detail by Ciancetta et al. (2017).

The DREAMS experiment package was equipped with its own battery (ABSL 18650NL Li-ion cells in 8s3p configuration), charged before launch.

11 CTPU and RTPU

Schiaparelli’s main computer was the Central Terminal Power Unit (CTPU), based around an Atmel AT697F Leon2-FT processor, including hibernation timer and 4 GBytes of mass memory, power distribution and thermal control for other units. During hibernation, the power consumption of the CTPU itself was <1 W, most of the electrical power being spent for thermal control.

The CTPU was housed inside the Central Bay. CAN (Controller Area Network) Bus interfaces linked the CTPU with the RTPU, RDA, UHF Transceiver and DREAMS. RS422

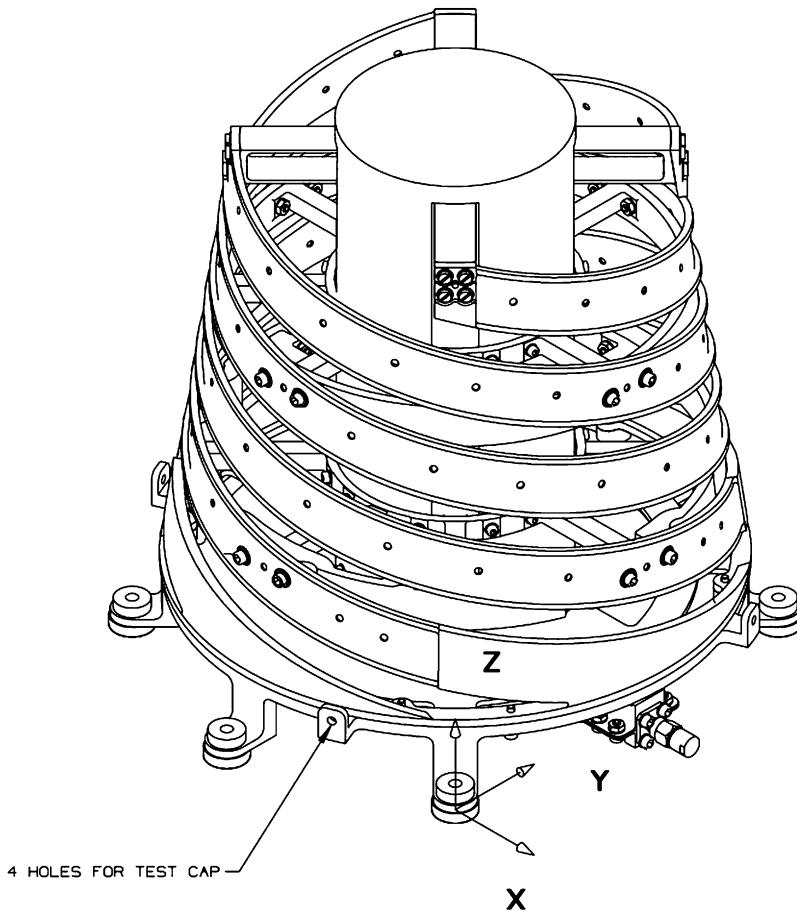


Fig. 14 Surface Platform UHF antenna (height 211.5 mm, base diameter 236 mm). Credit: Rymssa

interfaces linked the CTPU with the UHF Transceiver for TM/TC, the MIMU and DeCa. The data interface with the TGO was via MIL-1553. For EDL functions such as pyro and thruster valve control, interfaces to the Sun Detection Sensor, entry sensors, COMARS+ and RDA, a separate Remote Terminal and Power Unit (RTPU) was mounted on the underside of the baseplate. The RTPU was not intended to be used after touchdown.

The avionics block diagram (Fig. 13) shows the interconnections between the CTPU, RTPU and other units of Schiaparelli.

12 Telecommunications

Communications with TGO and the other Mars orbiters was by means of a UHF Transceiver (developed as an evolution of the design used on *Beagle 2*) and RF switch, feeding a patch antenna on the back cover (under an RF-transparent TPS patch) for entry and descent until Surface Platform separation, and a quad-helix antenna (Fig. 14) on top of the Surface Platform Central Bay, for the remaining portion of the descent, touchdown and surface phase.

Table 3 Planned telemetry sessions with Schiaparelli during separation, EDL and surface phases. Passes of Mars orbiters and carrier DTE (Direct To Earth) opportunities over the Schiaparelli landing site. MRO = Mars Reconnaissance Orbiter, MEX = *Mars Express*, MAV = MAVEN, ODY = *Mars Odyssey*. *Carrier only for landing survival verification, i.e. no data relay to Mars orbiters (but data transfer from DREAMS to CTPU still expected). Between these sessions the CTPU was set to be in hibernation, with DREAMS following its own measurement sequence (see Bettanini et al. 2018)

Orbiter/ DTE	Pass #	Time after nominal landing (19/10/2016 14:48:08 UTC)	Duration/ min:s
TGO	-	-3 days	15:00
TGO / DTE	0	-25 min	35:00
MRO	1	2.05 h	14:20
MRO	2	14.2 h	16:00
DTE	2	20.3 h	05:00*
MEX	3	26.3 h	15:30
MRO	3	26.3 h	15:30
MAV	1	29.4 h	42:00
ODY	1	30.5 h	04:10
MEX	3	33.2 h	17:00
MRO	4	38.5 h	14:40
DTE	3	48.2 h	05:00*
MEX	6	50.7 h	16:00
MRO	5	50.7 h	16:00
MRO	6	62.9 h	04:00
Etc. ...			

Transmission of real-time essential telemetry at 8 kbps was performed during EDL (TM being available from ~ 25 min before reaching the Entry Interface Point). This was received by the Electra telecommunications package on TGO. The low telemetry rate necessitated a selection of the most important parameters for transmission, sampled at 0.1 Hz, 1 Hz or 10 Hz depending on the parameter and mission sub-phase (higher rate data was stored on-board for transmission after touchdown). No interleaving was implemented to cope with the plasma black-out expected during entry, with the exception of an ‘event’ indication giving the maximum measured deceleration.

The carrier was also monitored by ESA’s *Mars Express* and the GMRT (Giant Metre-wave Radio Telescope) in Pune, India; see Esterhuizen et al. (2019).

Open-loop transmission was planned to continue during the touchdown phase until 15 min after landing, at which point the CTPU was planned to enter its first hibernation phase, having first activated DREAMS to begin its surface measurement phase.

For the surface relay phase, *Mars Odyssey*, *Mars Express*, MRO, MAVEN and TGO were all prepared to receive UHF transmission from Schiaparelli (see Edwards et al. 2017 for details), however TGO’s initial 4 sol, highly elliptical orbit after MOI limited its use for Schiaparelli post-landing to a single opportunity for open loop carrier monitoring. Passes were planned as shown in Table 3 until the estimated point that the DREAMS battery was to reach depletion; relay passes were defined thereafter according to orbiter availability until CTPU battery depletion including margin.

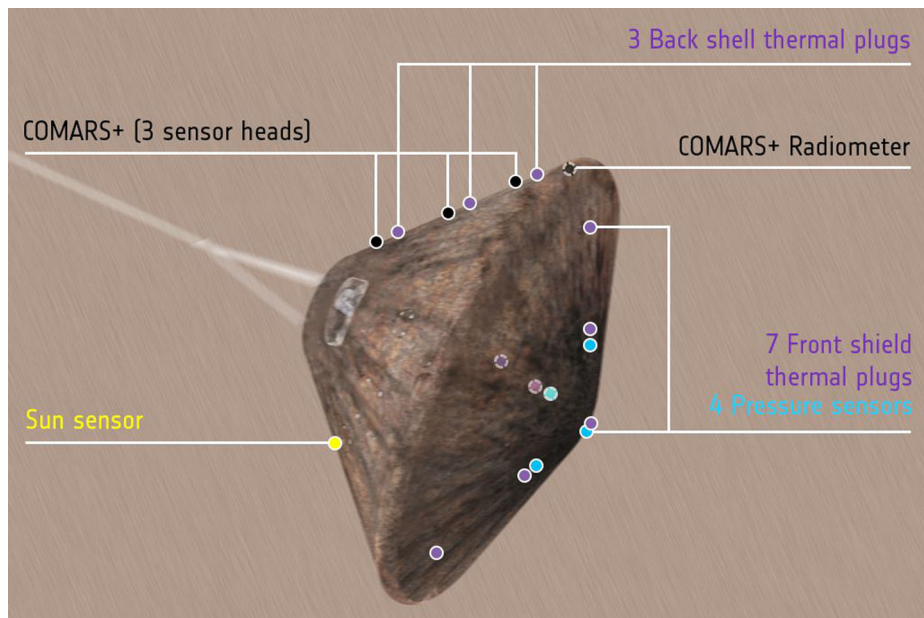


Fig. 15 Schematic layout of sensors on Schiaparelli heat shield. Copyright: ESA/ATG medialab

13 Payload Investigations

Although designed primarily as a technological demonstrator rather than as a platform for science, Schiaparelli carried a payload of experiments with total mass of approximately 15.2 kg (Table 4). The payload was a combination of: engineering sensors built into the vehicle, for heatshield monitoring during entry (Fig. 15) and for measuring the dynamics of the touchdown; sensors provided by ESA and national agencies, and experiments selected in response to an Announcement of Opportunity (released in November 2010) seeking proposals both for surface payload and for entry and descent science.

13.1 DREAMS

The DREAMS experiment package (‘Dust characterization, Risk assessment and Environment Analyser on the Martian Surface’) comprised six sensors plus associated electronics and battery (charged before launch). Two sensor masts were mounted on the top external surface of the Central Bay, for meteorological and electrical properties measurements, respectively. A further sensor for atmospheric pressure measurement was accommodated internally, with a tube protruding to the exterior to access the atmosphere. Communications with the CTPU were via a CAN Bus connection. DREAMS was planned to operate a timeline of measurement and data transfers to the CTPU during the surface phase, starting at touchdown. See Esposito et al. (2018) and Bettanini et al. (2018) for details.

13.2 DeCa

The Descent Camera (‘DeCa’) was supplied by ESA using a flight spare Visual Monitoring Camera from the Herschel-Planck project (VMC-HP), manufactured by OIP. Having been

Table 4 Schiaparelli Payload overview and masses

Location	Instrument/ Experiment/ Investigation	Quantity	Description	Mass/kg	Remarks
Front Shield	Pressure Sensors	4	Kulite XTL-DC-123C-190M-250-mBAR-A	4.590	Incl. mounting h/w and ~3 kg harness. See Pinaud et al. (2019), Schleutker et al. (2019) and Van Hove et al. (2019).
	Thermocouples	21	TC Direct Type J (3 per each of 7 thermal plugs embedded in TPS)		
	Thermistors	7	MEAS Pt200 internally at each thermal plug location		
Back Shell	Thermocouples	6	TC Direct Type J (2 per each of 3 thermal plugs)	3.110	Incl. mounting h/w and ~3 kg harness. See Pinaud et al. (2019).
	Thermistors	3	MEAS Pt200 internally at each thermal plug location		
-	COMARS+	3	Combined sensor heads for static pressure, total heat flux, temperature and two ICOTOM spectral radiometer sensors	1.731	Incl. instrument harness and e-box on internal surface of back cover. See Gülhan et al. (2018, 2019).
	AMELIA	1	Broadband IR Radiometer	-	See Ferri et al. (2019).
	DeCa	1	Science investigation using data from EDL sensors including IMU and RDA. VMC-HP FM#2 repurposed + mounting bracket	0.888	620 g camera unit + 268 g bracket. Excluding power & data harness. ~0.5 kg.
Surface Platform edge	Landing accelerometers	6	Endevco 2271 AM20; 3 orthogonal pairs (vertical and tangential) 120° apart, each sampled at 6 kHz with 12 bits and 0.159 g resolution over the range 1-400 g.	0.451	Each sensor 27 g, plus brackets and mounting at each location, and co-ax harness to CTPU
Surface Platform; Central Bay & Top of Central Bay	DREAMS	1	MetMast: - Mars Tem atmospheric temperature - MetWind wind velocity - DREAMS-H humidity - SIS Solar Irradiance Sensor	4.372	See Esposito et al. (2018) and Bettanini et al. (2018).
			DREAMS-P atmospheric pressure MicroARES electrical properties Common Electronics Unit (CEU) DREAMS Battery Optical retroreflector	0.055	Incl. 30 g attachment bracket (Deil' Agnello et al. 2017)
<i>Total</i>				<i>15.197</i>	

delivered to ESA in 2006 but not used for flight, it was available as an inventory item and selected for delta-qualification (using the VMC-HP EQM, which was also available and later incorporated into the EDM ATB), calibration, planetary protection cleaning and delivery for use on Schiaparelli.

The camera housing was $97 \times 97 \times 83.5 \text{ mm}^3$ (excluding the optics and connectors), with an electrical interface compatible with Schiaparelli's 28 V unregulated power supply. The Schiaparelli CTPU was equipped with a DS16 (RS422-like) serial data interface to receive the data from DeCa. The camera operated without telecommand, simply acquiring its sequence of images after power-on, the image data once acquired then being available for readout.

The objectives for DeCa were to obtain images of the martian surface in the vicinity of the landing area, and thus enable confirmation of the Surface Platform's attitude and position. Mounted on a dedicated bracket at the edge of the surface platform (see Fig. 11) with its optical axis angled 20° from the platform's +X axis, it was intended to acquire a sequence of 15 images of the martian terrain during descent, with 8-bit /pixel resolution. The time interval between images and the exposure time were pre-set to 1.5 s and 1 ms, respectively.

The image field of view through the fixed optics was $60^\circ \times 60^\circ$. Stored within the camera for as long as it is kept powered, the image data (one image cycle of 15 images corresponding to $3.76 \text{ Mb} = 3947640$ bytes of image data) was planned to be retrieved by the CTPU after touchdown for subsequent relay to ground. The detector is a Star-1000 APS sensor, of which the centre 512×512 pixels are used.

While the received housekeeping telemetry shows that image acquisition had started as planned, due to the EDL anomaly no images could be retrieved from the camera.

13.3 COMARS+

The COMARS+ sensor suite accommodated on the Back Shell operated during entry. See Gülhan et al. (2018, 2019) for details and results.

13.4 INRRI

A passive optical retroreflector was mounted on a bracket on top of the Surface Platform's Central Bay. See Dell'Agnello et al. (2017) for details.

13.5 AMELIA

The AMELIA team was selected to perform scientific analysis of the EDL data. See Aboudan et al. (2018) and Ferri et al. (2019).

14 Landing Site

The landing site of Schiaparelli was chosen by ESA early in the project (2009) based on engineering constraints alone. Meridiani Planum was selected as the safest (in terms of elevation and surface characteristics) known site having 'ground truth' characterisation (from the *Opportunity* rover).

The targeted site was at $6.10^\circ\text{W} / 2.05^\circ\text{S}$, at -1.45 km MOLA elevation. From mission analysis (including variation of arrival azimuth with the actual launch date within the window) and Monte Carlo simulation, a $3\text{-}\sigma$ ellipse of $110 \times 24 \text{ km}$ (major axes) was defined.

The atmospheric conditions were defined by the European Mars Climate Database (EMCD), a specific version of which (4.3.2) was generated for Schiaparelli. Knowledge of martian atmospheric conditions was also expected to be updated in the days prior to EDL with the help of data from other missions including MRO, *Mars Express* and *Opportunity*.

15 Touchdown & Surface Phases

The nominal duration of the surface phase was limited by the available energy from the on-board batteries, with some dependence on the thermal environment encountered by Schiaparelli at the landing site (with arrival at a Local Mean Solar Time (LMST) of 13:00). DREAMS' own battery would likely have become depleted before that of the CTPU, in which case Schiaparelli would have completed relay transmission of any remaining DREAMS data transferred to the CTPU prior to expiry of DREAMS, together with house-keeping data from the platform. After that, any remaining opportunities for relay would have been used to attempt repeat transmission of the data accumulated in memory.

Although in principle forward commanding of Schiaparelli during the surface phase would have been technically possible, this was not needed within the scope of the (few sols) nominal mission, and thus not planned.

16 Schiaparelli Model Philosophy

The design and verification of Schiaparelli required several development models to be built. The principal models were the Structural Model, the Drop Test Model, the Avionics Test Bench (ATB), and the Flight Model. These models and several others were used for design, development and co-ordinated analysis and testing with TGO according to mission phase and spacecraft configuration, as described in Table 5.

16.1 Structural Model

The main purpose of the Schiaparelli SM was to verify the mechanical properties of the vehicle's main structural elements – back shell, front shield and surface platform, and the interfaces among them. The SM was subjected to sine testing, entry load static test and parachute deployment static load test. The SM was also used to perform leak testing of the bioseal and to verify DHMR compatibility of the main structural parts.

16.2 Surface Platform Drop Test Model

The purpose of this model was to test the platform's robustness to landing scenarios (velocity and surface characteristics), in particular with the crushable material for damping the final touchdown (del Campo et al. 2016).

16.3 Avionics Test Bench

This bench-top model was used to verify the electrical and digital interfaces between the various elements of Schiaparelli, and to test the on-board software.

16.4 Flight Model

This was the only complete model of Schiaparelli assembled (Fig. 16). Flight spares of some elements were available in case of need.

Table 5 Verification activities carried out for the various Schiaparelli EDM functions and mission phases

Mission phase	Key relevant EDM functions	Key, relevant verification activities
<i>Ground:</i> assembly and test, and Launch Campaign	Planetary protection	Clean activities carried out inside ISO7HC clean room or clean tent with all personnel in full bunny-suits following strict contamination and bioburden control protocols. EDM parts and materials qualified for DHMR and cleaning with IPA. Activities outside ISO7HC only with heat shield closed and interior of EDM protected by bioseal, covers, HEPA filter or venting box. EDM (re-)cleaning with IPA.
<i>Launch:</i>	EDM part of SCC, and OFF	Bioseal was qualified, and periodically re-verified with dedicated leak testing.
<i>Cruise:</i>	EDM part of SCC, thermal control by TGO, activated for health checks	Mechanical environment structural qualification of the EDM design with sine testing of EDM SM; Mechanical environment PFM acceptance by testing SCC in both sine and acoustic regimes (EDM on top of TGO). TGO functions for control of EDM tested on TGO ATB, and during TGO TVAC.
<i>Separation:</i>	MSA	Dedicated MSA qualification tests with simulated TGO and EDM.
<i>Coast:</i>	Pre-separation thermal boost	Thermal boost test during EDM
<i>EDL:</i>	Hibernation, post-hibernation heating, GNC (STR, IMU)	Hibernation was tested on ATB, and abbreviated test in EDM PFM TVAC; Mission Simulation Test (MST) carried out on ATB
	GNC (MIMU, RDA)	MST carried out on ATB, and PFM; RDA verification with signal simulator and field testing
	UHF telecommunications	UHF transponder compatibility with TGO and other orbiters tested against TTC system of those spacecraft's ATB; EDM self-compatibility of UHF tested during cruise; Antennas (BCV patch and LP quad-helix) tested at unit level and for signal continuity.
Atmospheric deceleration	Heat shield,	EDL validation with dedicated end-to-end simulation package. Development tests with arc jet facility; coupon tests; Static test of EDM structure to withstand atmospheric deceleration compressive loads using EDM SM and dedicated test facility.
	COMARS+	See Gülhan et al. (2018)

Table 5 (Continued)

Mission phase	Key relevant EDM functions	Key, relevant verification activities
Parachute descent	Parachute system	Sub-scale wind-tunnel development testing; full-scale wind-tunnel qualification testing for dynamic loads and deployment sequence.
Powered descent	Propulsion system, DeCa	Static test of EDM structure to withstand parachute loads using EDM SM. Hot firing test of engine set; dedicated partial propulsion system model built to test valve control logic; Delta-qualification vs. VMC-HP for EMC, quasi-static loads and temperature range.
Landing Surface:	Crushable structure DREAMS	Drop testing with dedicated LP model, correlated with FEM simulations; see del Campo et al. (2016). Thermal validation test of Central Bay; Battery thermal testing and qualification to determine lifetime; MST carried out on ATB and on PFM.

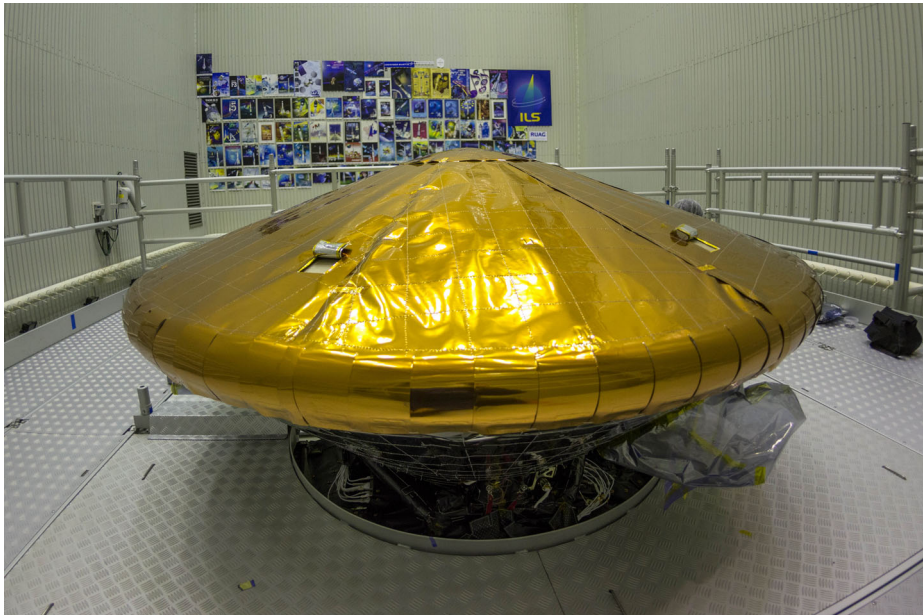


Fig. 16 View of Schiaparelli at Baikonur after mounting to the TGO, showing installation of the FS MLI (visible open flaps – closed soon after this photo was taken – were for access to the ground handling points). Copyright: ESA - B. Bethge

17 Launch, Cruise, Commissioning and Check-Outs

During launch (and most of the cruise), Schiaparelli was passive except for thermal control from the TGO, via the RTPU ('EDM Service Mode').

Following launch on a Proton-M on 14 March 2016, ExoMars 2016 experienced a nominal 7-month cruise to Mars, including two Deep-Space Manoeuvres. Following these, two small Trajectory Correction Manoeuvres were performed. A possible third and final TCM was not performed due to the near-perfect navigation achieved. See Pellegrinetti et al. (2019) for details of the flight dynamics operations and targeting for EDL.

During cruise, Schiaparelli was commissioned and in-flight check-outs and battery charging performed, with total duration of 55.7 hours. Figure 17 shows the cumulative duration of CTPU operations. Commissioning and calibration for the pre-separation thermal boost were performed in the period 8-21 April 2016. Mid-cruise checkout was performed in the period 16-23 June 2016. A third set of checkouts was performed 8-21 Sept 2016, with preparations for separation beginning 28 Sept 2016.

High disturbance torques were detected when Schiaparelli was exposed to the Sun during a slew early during cruise (triggering an autonomous TGO reaction wheel unloading). Following further outgassing characterisation slews (also needed for TGO), some of the torques were indeed attributed to outgassing from Schiaparelli (perhaps from absorbed moisture in the TPS). Baking operations (slews to illuminate different faces of the spacecraft) were performed during mid-cruise (26 May to 4 July 2016) until the torques had reduced to an insignificant level.

Separation of Schiaparelli occurred nominally on 16 October 2016, 3 days before Mars arrival (note: the date of Mars arrival was fixed before launch, independent of the actual

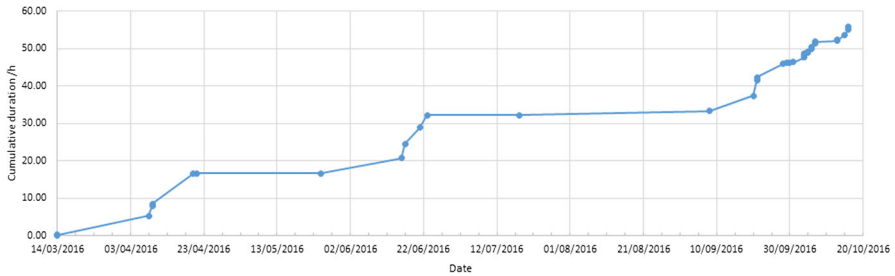


Fig. 17 Cumulative duration of Schiaparelli CTPU operation during cruise

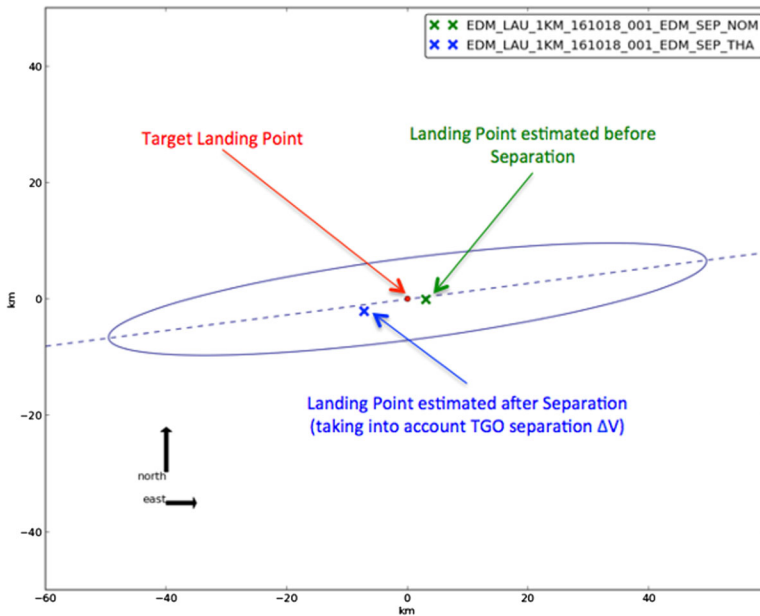


Fig. 18 Schiaparelli estimated landing point w.r.t. target, before and after separation from TGO. Entry was prograde, from west to east

launch date within the 2016 launch window). Telemetry for nearly 19 min around separation was received from Schiaparelli during this phase by the Electra UHF relay on TGO, operating in open-loop recording mode.

As reported by Bonetti et al. (2018), it was found from reconstruction of the separation velocity from IMU data that there was an over-performance of the spring-based separation system (delta absolute axial velocity of 335 mm s^{-1} vs. 320 mm s^{-1} , corresponding to a 5.4σ value), while the roll rate was slightly lower than expected (2.617 rpm vs. 2.70 rpm , a 1.5σ value). Nevertheless the estimated Entry Interface Point (EIP) and landing point (Fig. 18) were well within the predictions.

Nominal entry of Schiaparelli into its 3-day hibernation occurred 15 min after separation, with all on-board systems having operated nominally.

Wake-up from hibernation mode occurred nominally on 19 October 2016, 75 min before EIP. All on-board systems operated nominally when exiting the hibernation mode, and the

thermal environment inside Schiaparelli during the hibernation phase was fully in line with expectations.

See Portigliotti et al. (2017) and Bonetti et al. (2018) for a post-flight analysis of the Schiaparelli coasting, entry and descent, and Pinaud et al. (2019) and Gülhan et al. (2019) for post-flight analyses of data from the heat shield sensors and COMARS+, respectively.

As is now well known, an anomaly occurred due to a mismatch between the IMU angular rate saturation behaviour at parachute deployment, and how such saturation was handled by the GNC algorithm once data from the RDA was brought into the control loop. This caused premature separation of the Surface Platform from the Back Shell, a short RCS propulsive phase (~ 3 s priming phase to reduce the angular rates, vs. the expected nominal design duration of 28.5 s), and transition to the touchdown phase (including activation of DREAMS, as shown by receipt on ground of a first housekeeping packet from the experiment). Although sadly neither DeCa nor DREAMS were able to return science data, much was learned from the real-time telemetry about the functioning of Schiaparelli and the measurements made during entry and descent for analysis by the COMARS+ and AMELIA teams.

With respect to the nominal prediction of 2.8 Mbit EDL essential data transmitted, once the blackout duration (about 72 s) and shorter-than-nominal descent phase are taken into account, the telemetry actually received on ground amounts to some 2/3 of the prediction. The total amount of data expected in the nominal mission (for the full EDL data set plus science and engineering data from the coasting, EDL and nominal surface phases) was 207 Mbit.

See Tolker-Nielsen (2017) for the report of the anomaly enquiry.

Appendix: Schiaparelli Industrial Partners & Suppliers

- Thales-Alenia Space Italy (TAS-I): Prime Contractor (Turin), CTPU prime (Milan), Radar Doppler Altimeter prime (Rome)
- Thales-Alenia Space France (TAS-F): Entry & Descent System Lead; Back Cover Structure, Reaction Control System, TVTB test
- Airbus Defence & Space France (Bordeaux): Heatshield, TPS
- Airbus Defence & Space (Germany): RCS engine assembly, pyrovalves
- EADS CASA Espacio (Spain): harness
- Sener (Spain): Front Shield Separation Mechanism, Surface Platform Structure and Separation Mechanism
- RUAG Space (Switzerland): Main Separation Assembly
- Aerosekur (Italy): Parachute, HEPA filter
- Selex Galileo (Italy): CTPU Electrical Power Board
- General Dynamics (USA): Parachute Deployment Device
- Honeywell (USA): MIMU
- ABSL (UK): Batteries
- HPS (Portugal): thermal blanket
- QinetiQ (UK): UHF Transceiver
- TERMA (Denmark): RTPU
- TNO-TPD (Netherlands): Sun Detection Sensor
- Haigh-Farr (USA): UHF Antenna on Back Cover
- RYMSA (Spain): Surface Platform UHF Antenna
- Rafael (Israel): RCS propellant tanks
- ATK (USA): RCS He pressurant tank
- Moog (UK): RCS valves

- ERG Aerospace (USA): thermal capacitors
- Gerling, Holz & Co (Germany): RCS consumables
- Sofrance (France): RCS pressurant and propellant filter
- Bradford (Netherlands): RCS pressure transducers
- Cobham (USA): RCS pyrovalves
- SMC (USA): RCS pressure regulator
- M&I Materials Ltd (UK): WolfMet tungsten alloy ballast/balance masses
- GMV (Spain): GNC software
- Vorticity (UK): parachute system engineering support
- Deimos (Spain): mission analysis support
- Fluid Gravity Engineering (UK): aerothermal analysis engineering support
- LMD (France): Mars atmosphere characterisation
- IRSPS (Italy): Mars terrain characterisation

Acknowledgements The authors wish to thank ESA colleagues T. Walloschek, C. Alary, S. Langlois, H.-J. von der Hardt, A. Winton, L. Bolognino and D. Koschny for information and insight provided for this paper, and S. Portigliotti from TAS-I Torino for clarifications. A.J. Ball also wishes to thank H. Svedhem for his patience and encouragement, and the reviewers for their helpful suggestions.

Open Access This article is licensed under a Creative Commons Attribution 4.0 International License, which permits use, sharing, adaptation, distribution and reproduction in any medium or format, as long as you give appropriate credit to the original author(s) and the source, provide a link to the Creative Commons licence, and indicate if changes were made. The images or other third party material in this article are included in the article's Creative Commons licence, unless indicated otherwise in a credit line to the material. If material is not included in the article's Creative Commons licence and your intended use is not permitted by statutory regulation or exceeds the permitted use, you will need to obtain permission directly from the copyright holder. To view a copy of this licence, visit <http://creativecommons.org/licenses/by/4.0/>.

References

- A. Aboudan, G. Colombatti, C. Bettanini, F. Ferri, S. Lewis, B. Van Hove, Ö. Karatekin, S. Debei, ExoMars 2016 Schiaparelli module trajectory and atmospheric profiles reconstruction. *Space Sci. Rev.* **214**, 97 (2018). <https://doi.org/10.1007/s11214-018-0532-3>
- A. Amelio, S. Portigliotti, M. Montagna, G. Palermo, F. Rame, G. Passarelli, D. Grana, O. Bayle, T. Blancquaert, D. Sanchez, D. Temperanza, L. Lorenzoni, ExoMars 2016 entry descent and landing module avionics and GNC architecture and their validation, in *DASIA 2016, Proceedings of the Conference Held 10-12 May, 2016 at Tallinn in Estonia*, ed. by L.O. Ouwehand. ESA-SP, vol. 736 (2016). ISBN 978-92-9221-301-5. id. 16
- C. Bettanini, F. Esposito, S. Debei et al., The DREAMS experiment flown on the ExoMars 2016 mission for the study of Martian environment during the dust storm season. *Measurement* **122**, 484–493 (2018). <https://doi.org/10.1016/j.measurement.2018.01.019>
- O. Bombaci, M. Iorio, P. Pepe, ExoMars Radar Doppler Altimeter (a Doppler radar for accurate attitude measurements in support to landing phase), in *2016 IEEE Metrology for Aerospace (MetroAeroSpace)* (2016), pp. 65–70. <https://doi.org/10.1109/MetroAeroSpace.2016.7573187>
- D. Bonetti, G. De Zaiacomo, G. Blanco, I. Pontijas Fuentes, S. Portigliotti, O. Bayle, L. Lorenzoni, ExoMars 2016: Schiaparelli coasting, entry and descent post flight mission analysis. *Acta Astronaut.* **149**, 93–105 (2018). <https://doi.org/10.1016/j.actaastro.2018.05.029>
- L. Caldirola, B. Schmid, M. Cattaneo, A. Schiaffini, ExoMars MSA. “Test HDRM” development for separation performance verification, in *Proc. 16th European Space Mechanisms and Tribology Symposium*, Bilbao, Spain, 23–25 September 2015, ed. by L. Ouwehand. ESA-SP, vol. 737 (2015)
- E. Ciancetta, G. Cuzzocrea, J.-J. Digoïn, F. Chiusano, ExoMars 2016 mission Electrical Power System, in *European Space Power Conference 2016, E3S Web of Conferences*, vol. 16 (2017), p. 13012. <https://doi.org/10.1051/e3sconf/20171613012>
- F. del Campo, Y.E. Jauregui, R. Haya Ramos, ExoMars 2016 Landing Impact Verification, in 13th Interplanetary Probe Workshop, Laurel, Maryland, USA, June 13-17 2016

- C. Davies and M. Arcadi (eds.), Planetary Mission Entry Vehicles Quick Reference Guide. Version 3.0, NASA/SP-2006-3401 (2006). <https://ntrs.nasa.gov/citations/20070022789>
- S. Dell'Agnello, G. Delle Monache, L. Porcelli, A. Boni, S. Contessa, E. Ciocci, M. Martini, M. Tibuzzi, N. Intaglietta, L. Salvatori, P. Tuscano, G. Patrizi, C. Mondaini, C. Lops, R. Vittori, M. Maiello, E. Flamini, E. Marchetti, G. Bianco, R. Mugnuolo, C. Cantone, INRRI-EDM/2016: the first laser retroreflector on the surface of Mars. *Adv. Space Res.* **59**(2), 645–655 (2017). <https://doi.org/10.1016/j.asr.2016.10.011>
- C.D. Edwards, S. Asmar, K.N. Bruvold, N.F. Chamberlain, S. Esterhuizen, R.E. Gladden, M.D. Johnston, I. Kuperman, R. Mendoza, C.L. Potts, M.P. Pugh, D. Wenkert, M. Denis, P. Schmitz, S. Wood, O. Bayle, A. Winton, M. Montagna, Relay communications support to the ExoMars Schiaparelli Lander, in IEEE Aerospace Conference, Big Sky MT, 4–11 March 2017. <https://doi.org/10.1109/AERO.2017.7943620>
- F. Esposito, S. Debei, C. Bettanini et al., The DREAMS experiment onboard the Schiaparelli module of the ExoMars 2016 mission: design, performances and expected results. *Space Sci. Rev.* **214**(6), 103 (2018). <https://doi.org/10.1007/s11214-018-0535-0>
- S. Esterhuizen, S.W. Asmar, K. De, Y. Gupta, S.N. Katore, B. Ajithkumar, ExoMars Schiaparelli direct-to-Earth observation using GMRT. *Radio Sci.* **54**(3), 314–325 (2019). <https://doi.org/10.1029/2018RS006707>
- F. Ferri, Ö. Karatekin, S.R. Lewis et al., ExoMars atmospheric Mars entry and landing investigations and analysis (AMELIA). *Space Sci. Rev.* **215**(1), 8 (2019). <https://doi.org/10.1007/s11214-019-0578-x>
- M. Gottero, V. Perotto, R. Martino, C. Alary, S. Lapensée, PFM Thermal balance-thermal cycling test of the ExoMars Entry Descent and Landing Demonstrator Module, in 46th International Conference on Environmental Systems, Vienna, Austria, 10–14 July 2016. ICES-2016-248
- M. Gottero, V. Perotto, R. Martino, B. Leyda, B. Ozmat, Phase-change thermal capacitors for ExoMars 2016 mission, in 44th International Conference on Environmental Systems, Tucson AZ, USA, 13–17, July 2014. ICES-2014-147
- A. Gülhan, T. Thiele, F. Siebe, R. Kronen, Combined instrumentation package COMARS+ for the ExoMars Schiaparelli lander. *Space Sci. Rev.* **214**(1), 12 (2018). <https://doi.org/10.1007/s11214-017-0447-4>
- A. Gülhan, T. Thiele, F. Siebe, R. Kronen, T. Schleutker, Aerothermal measurements from the ExoMars Schiaparelli capsule entry. *J. Spacecr. Rockets* **56**(1), 68–81 (2019). <https://doi.org/10.2514/1.A34228>
- D. Pellegrinetti, R. Guilanyà, P. Muñoz, R. Vidal, E. Basso, J. Schwartz, U. Herfort, ExoMars 2016 – flight dynamics operations for the targeting of the Schiaparelli module entry descent and landing and the Trace Gas Orbiter Mars orbit insertion, in 27th International Symposium on Space Flight Dynamics, Australia, 24–28 February 2019
- V. Perotto, M. Gottero, R. Martino, C. Alary, In-flight verification of the Thermal Control System of ExoMars EDM, in 47th International Conference on Environmental Systems, Charleston SC, USA, 16–20 July 2017. ICES-2017-304
- G. Pinaud, J. Bertrand, J. Soler, P. Tran, H. Ritter, O. Bayle, ExoMars mission 2016: a preliminary post-flight performance analysis of the heat shield during entry on Mars atmosphere, in: AIAA Scitech Forum, San Diego, 7–11 January 2019. <https://doi.org/10.2514/6.2019-0244>
- S. Portigliotti, C. Cassi, M. Montagna, P. Martella, M. Faletta, L. Boi, S. De Sanctis, D. Granà, O. Bayle, T. Blancquaert, L. Lorenzoni, ExoMars 2016, the Schiaparelli mission. EDL demonstration results from real time telemetry before unfortunate impact. Presented at the 14th International Planetary Probe Workshop, the Hague, 12–16 June 2017
- M. Prieto, F. del Campo, Y.E. Jauregui, G. Biondetti, T. Walloschek, Separation mechanisms and release/motion analysis for ExoMars 2016, in *Proc. 15th European Space Mechanisms and Tribology Symposium*, Noordwijk, The Netherlands, 25–27 September 2013, ed. by L. Ouwehand. ESA-SP, vol. 718 (2013)
- T. Schleutker, A. Gülhan, B. Van Hove, Ö. Karatekin, ExoMars flush air data system: experimental and numerical investigation. *J. Spacecr. Rockets* **56**(4), 971–982 (2019). <https://doi.org/10.2514/1.A34185>
- T. Tolker-Nielsen, *ExoMars 2016 – Schiaparelli Anomaly Enquiry. DG-I/2017/546/TTN Iss. 1, Rev. 0* (European Space Agency, Paris, 2017). <https://exploration.esa.int/web/mars/-/59176-exomars-2016-schiaparelli-anomaly-inquiry>
- B. Van Hove, Ö. Karatekin, T. Schleutker, A. Gülhan, ExoMars flush air data system: entry simulation and atmospheric reconstruction method. *J. Spacecr. Rockets* **56**(4), 1205–1220 (2019). <https://doi.org/10.2514/1.A34187>